ARTICLE NO. 79-1561R

J80-229

Prediction of Two- and Three-Dimensional Asymmetrical Turbulent Wakes, Including Curvature and Rotation Effects

20005
20007
60001

C. Hah* and B. Lakshminarayana†
The Pennsylvania State University, University Park, Pa.

Two- and three-dimensional turbulent wakes which develop under the influence of streamline curvature and rotation were calculated with three turbulence closure models. The first model was comprised of transport equations for the turbulent kinetic energy and the rate of energy dissipation. The second model was comprised of equations for the rate of turbulent kinetic energy dissipation and Reynolds stresses, but the effects of the convection and diffusion in the Reynolds stress transport equation were handled collectively. The third model utilizes equations of turbulent kinetic energy dissipation and Reynolds stresses in nearly exact form. All three of the models were modified for the effects of streamline curvature. The second and third models include the effects of rotation through the rotation-originated redistribution term in the transport equation of Reynolds stresses. The numerical results for the wakes of airfoils, cascades, and turbomachinery rotor blades demonstrate that the second and third models provide accurate predictions, but computer time and storage can be considerably saved with the second model.

Nomenclature

C = chord length of blade
$C_1, C_s, C_{\phi 1}, C_\epsilon$, $C_{\epsilon 1}, C_{\epsilon 2}, \gamma, C_c$ = constants in turbulence closure models
g_{ij}, g^{ij} = metric tensor [Eq. (13)]
k = turbulence kinetic energy
P = $\overline{u_i u_j} U^i{}_{,j}$
p = static pressure
p' = fluctuating component of static pressure
p^* = reduced static pressure $[p - (\rho/2) r^2 \Omega^2]$
S = blade spacing (Fig. 6)
S_1, S_2, S_3 = various forms of the source term in the energy dissipation equation
s,r,b = curvilinear coordinates (streamwise, normal, and radial direction, Fig. 1; $s=0$, $r=0$ is at the trailing edge of blade)
s,n,r = streamwise, normal, and radial directions for rotor wake (Fig. 11)
U,V,W = streamwise, normal, and spanwise mean velocities (Figs. 1, 6, and 11)
u,v,w = fluctuating velocities in streamwise, normal, and spanwise velocities (Figs. 1, 6, and 11)
U^i, u^i = contravariant mean and fluctuating velocity component [U,V,W,u,v,w in (s,r,b) coordinates]
R_i = Richardson number for the curved turbulent flow
$\overline{u^i u^i}$ = turbulence intensity with components $\overline{u^2}$, $\overline{v^2}, \overline{w^2}$, in s,r,b directions
$\overline{u^i u^j}$ = shear stress with components $\overline{uv}$, $\overline{uw}$, and $\overline{vw}$ in (s,r,b) coordinates
Ω = angular speed of rotor
Ω_i = angular velocity of rotor [$\Omega_s, \Omega_n, \Omega_r$ in (s,n,r) coordinates]
β = angle between machine axis and streamwise direction (Fig. 11)
δ_{ij} = Kronecker delta
$\epsilon_{ijk}, \epsilon^{ijk}$ = permutation tensor
ν = kinetic viscosity
ρ = density
Γ^i_{jk} = Christoffel symbol of second kind

Subscripts

∞ = values in the freestream
s,r,b = streamwise, normal, and radial components, respectively (Fig. 1)
t = values at blade tip
c = values at wake center

Superscripts

$\overline{\ }$ = average value
$(\ )'$ = fluctuating quantity

Presented as Paper 79-1561 at the AIAA 12th Fluid and Plasma Dynamics Conference, Williamsburg, Va., July 23-25, 1979; submitted Sept. 18, 1979; revision received Feb. 26, 1980.

Index categories: Computational Methods; Jets, Wakes, and Viscid-Inviscid Flow Interactions; Air-Breathing Propulsion.

*Research Associate, Dept. of Aerospace Engineering. Member AIAA.

†Professor, Dept. of Aerospace Engineering. Associate Fellow AIAA.

Introduction

THE turbulence structure of the wake developing under the influence of streamline curvature and rotation is different from that of the wake without these effects. For accurate prediction of turbulent wakes, the effects of curvature and rotation should be accounted for properly in the turbulence closure models for the governing equations. A detailed comparison of various turbulence models for wakes without the effects of curvature and rotation has been given by Launder et al.[1] and Pope and Whitelaw.[2] Therefore, the present study will concentrate on modeling for the effects of curvature and rotation.

The effects of streamline curvature in a turbulent flow were first recognized by Prandtl,[3] and many investigations have been carried out since then. Experimental investigations (e.g., Patel,[4] So and Mellor,[5] and Castro and Bradshaw[6]) have shown that the turbulence structure, as well as the mean velocity profile, is changed considerably due to the effects of streamline curvature. The measurements in the turbulent wakes of a single airfoil at various incidence angles by Hah and Lakshminarayana[7] showed that the decay rates of mean velocity and Reynolds stresses depend on the streamline curvature. A comprehensive review on the effects of streamline curvature in the turbulent flow is given by Bradshaw.[8] Various proposals to include the effects of streamline curvature in the modeling of turbulent flow have been made. Prandtl[3] suggested a modification of mixing-length theory. So[9] proposed a turbulent velocity scale for curved shear flows. Bradshaw[10] incorporated the effects of

streamline curvature by using the mixing-length concept and the analogy between buoyancy and curvature effects. Launder et al.[11] modified the two-equation turbulence closure model for the effects of streamline curvature.

Extensive data were recently reported[13-15] on the wake affected by rotation; but very few theoretical investigations have been made that fully account for the effects of rotation. A comprehensive review on the effects of rotation is given by Johnston.[12] Experimental investigations by Raj and Lakshminarayana,[13] Reynolds et al.,[14] and Ravindranath and Lakshminarayana[15] have shown very high radial intensity in the wake of rotating blades. This high radial intensity is due to the effects of rotation on the turbulence structure. Majumdar et al.[16] used the two-equation turbulence closure model for the calculation of the flow in the rotating duct and reported that their predictions were not quite satisfactory at high rotational speed.

The objective of this discussion is to compare the performance of three different turbulence closure models for the effects of streamline curvature and rotation. The first model comprised two transport equations for the turbulent kinetic energy and the rate of turbulent energy dissipation. The second and third models use the transport equations of Reynolds stresses and the rate of turbulent kinetic energy dissipation. In the second model, the diffusion and convection terms in the Reynolds stress transport equations are handled collectively. All three models were further modified for the effects of streamline curvature. The effects of rotation were included in the second and third models through the rotation-originated redistribution term in the transport equations of Reynolds stresses on the rotating curvilinear coordinate system.

Governing Equations

The equations governing the steady, incompressible, and fully turbulent flow relative to a coordinate system rotating with angular velocity Ω_i are introduced in generalized tensor form.

The continuity and momentum equations are, respectively,

$$U^i{}_{,i}=0, \quad u^i{}_{,i}=0 \tag{1}$$

$$U^j U^i{}_{,j}+\overline{u^j u^i}_{,j}+2\epsilon^{ijk}\Omega_j U_k=-\frac{g^{ij}}{\rho}\frac{\partial p^*}{\partial x^j}+\nu g_{jk}U^i{}_{,jk} \tag{2}$$

where U^i, u^i are mean and fluctuating contravariant velocity components.

The transport equations for the turbulence closure which make up the three turbulent closure models are as follows.

First model: two-equation model

$$U^i\frac{\partial k}{\partial x^i}=\frac{\partial}{\partial x^i}\left(\frac{\nu_{\text{eff}}}{\sigma_k}\frac{\partial k}{\partial x^i}\right)+P-\epsilon \tag{3}$$

$$U^i\frac{\partial \epsilon}{\partial x^i}=\frac{\partial}{\partial x^i}\left(\frac{\nu_{\text{eff}}}{\sigma_\epsilon}\frac{\partial \epsilon}{\partial x^i}\right)+S-C_{\epsilon 2}\frac{\epsilon^2}{k} \tag{4}$$

where

$$\nu_{\text{eff}}=C_\mu k^2/\epsilon, \quad P=-\overline{u_i u_j}U^i{}_{,j}, \quad k=\tfrac{1}{2}g_{ij}\overline{u^i u^j}$$

$$-\overline{u^i u^j}=\nu_{\text{eff}}(U^i{}_{,j}+U^j{}_{,i})-\tfrac{2}{3}kg^{ij}$$

and S is the source term in the transport equation of the rate of turbulent kinetic energy dissipation. Two forms of S were utilized and the results with each form were analyzed. The two forms of S are

$$S_1=C_{\epsilon 1}(\epsilon/k)P \tag{5a}$$

and

$$S_2=C_\ell\frac{\epsilon^2}{k^3}(\overline{u^i u^j}-\tfrac{2}{3}k\delta_{ij})(\overline{u^j u^i}-\tfrac{2}{3}k\delta_{ji}) \tag{5b}$$

Second and third models: Reynolds stress models. The second and third models utilize the simplified form of the transport equations of Reynolds stress. The pressure-strain correlation term in the transport equation of Reynolds stress is modeled following the proposals by Rotta[17] and Naot et al.[18] Furthermore, the rate of turbulence energy production, which appears in the modeling of mean-strain effects in the pressure-strain correlation is replaced with the rate of turbulent kinetic energy dissipation. The second and third models differ only in the handling of convection and diffusion terms. The convection and diffusion terms are handled collectively in the second model; the effects of the two terms are assumed to be proportional to the production term and the magnitude of the effects is corrected at each iteration.

The third model includes the individual effects of convection and diffusion and is similar to the equation used by Launder et al.[1] for straight nonrotating flows. But the rotation-originated redistribution term was added in the turbulence closure equation.

Second model: simplified Reynolds stress model. The equation used for this case is given by Hah and Lakshminarayana[19]

$$0=(1+C_1)(-\overline{u_k u^j}U^i{}_{,k}-\overline{u_k u^i}U^j{}_{,k})(1-\gamma)-2(\epsilon^{ilm}\Omega_l\overline{u_m u^j}+\epsilon^{jlm}\Omega_l\overline{u_m u^i})-\tfrac{2}{3}g^{ij}\epsilon(1-\gamma)-C_{\phi 1}(\epsilon/k)(\overline{u^i u^j}-\tfrac{2}{3}g^{ij}k) \tag{6}$$

where C_1 relates the collective effects of the convection and diffusion terms to the production terms, and γ is constant related to the pressure-strain correlation due to the presence of mean strain rate.

Third model: full Reynolds stress equations. The complete Reynolds stress equation (with suitable modeling for pressure-velocity correlation, etc.) is given as follows[19]

$$U^k\overline{u^i u^j}_{,k}=[C_s(k/\epsilon)\overline{u_k u_m}(\overline{u^i u^j})_{,m}]_{,k}+(-\overline{u_k u^j}U^i{}_{,k}-\overline{u_k u^i}U^j{}_{,k})(1-\gamma)-2(\epsilon^{ilm}\Omega_l\overline{u_m u^j}+\epsilon^{jlm}\Omega_l\overline{u_m u^i})-\tfrac{2}{3}g^{ij}\epsilon(1-\gamma)-C_{\phi 1}(\epsilon/k)(\overline{u^i u^j}-\tfrac{2}{3}g^{ij}k) \tag{7}$$

The values of constants in Eqs. (3-7) were not optimized for the present curved wakes; the values used by Pope and Whitelaw[2] were adopted. A value of 1.8 for C_ℓ in Eq. (5) was used in the present calculation.

Various turbulence models used in this investigation are tabulated in Table 1. Nine different turbulence models, shown in Table 1, were evaluated for the prediction of isolated airfoil, cascade and rotor wakes.

Modification of Turbulence Closure Models for Effects of Streamline Curvature and Rotation

The effect of streamline curvature on a fluid flow has been qualitatively explained with the motion of a disturbed element of fluid. The argument based on incompressible, inviscid fluid is as follows. The effect of streamline curvature is to stabilize the flowfield and consequently diminish the turbulent transportation when the angular momentum increases with the radius of streamline curvature and vice versa for the opposite case. Quantitatively, the following expression can be derived for the criterion of stability

$$\omega^2=2\frac{U}{r^2}\frac{\mathrm{d}}{\mathrm{d}r}(Ur)=2\left(\frac{U}{r}\frac{\mathrm{d}U}{\mathrm{d}r}+\frac{U^2}{r^2}\right) \tag{8}$$

where ω is the corresponding frequency, U circumferential velocity component and r the radius of curvature. The

Table 1 Turbulence closure models with different forms of source term in the equation for rate of turbulent kinetic energy dissipation

	Source term in the dissipation Eq. (4)		
Turbulence models	S_1	S_2	S_3
$k-\epsilon$ [Eqs. (3) and (4)]	$k\epsilon 1$	$k\epsilon 2$	$k\epsilon 3$
Modified Reynolds stress [Eqs. (3), (4), and (6)]	MRSM1	MRSM2	MRSM3
Reynolds stress [Eqs. (4) and (7)]	RSM1	RSM2	RSM3

flowfield is stabilized by streamline curvature when ω has a real value. For most thin shear flow, the first term is dominant. The turbulence closure models with the conventional dissipation equation [with the source term, Eq. (5a)] have been widely applied and criticized for poor prediction of curved flows (e.g., Refs. 8 and 11).

The existing prediction techniques for curved turbulent flow utilizing the turbulence models with the conventional dissipation equation [with the source term, Eq. (5a)] are considered to be inadequate. This is caused by the inappropriate form of the dissipation equation which is based on unproven assumptions and tested with only straight flows.

To represent the effect of streamline curvature properly, the rate of energy dissipation should be increased where the angular momentum increases with the radius of curvature and decreased where the angular momentum decreases with the radius of curvature. For the coordinate system shown in Fig. 1, the production term in Eq. (3) is, neglecting high-order stress terms,

$$P=-\overline{u_iu_j}U^i{}_{,j}=-\overline{u^2}\left(\frac{\partial U}{\partial s}+U\frac{s}{r^2}+V\frac{s^2}{r^3}\right)$$
$$-\overline{v^2}\left(\frac{\partial V}{\partial r}+U\frac{s}{r^2}-V\frac{s^2}{r^3}\right)$$
$$-\overline{uv}\left(\frac{\partial U}{\partial r}+\frac{\partial V}{\partial s}-\frac{U}{r}+U\frac{s^2}{r^3}+V\frac{s}{r^2}-V\frac{s^3}{r^4}\right) \tag{9}$$

and if higher order curvature terms including s/r^2 are neglected,

$$P=-\overline{u^2}\frac{\partial U}{\partial s}-\overline{v^2}\frac{\partial V}{\partial r}-\overline{uv}\left(\frac{\partial U}{\partial r}+\frac{\partial V}{\partial s}-\frac{U}{r}\right)$$

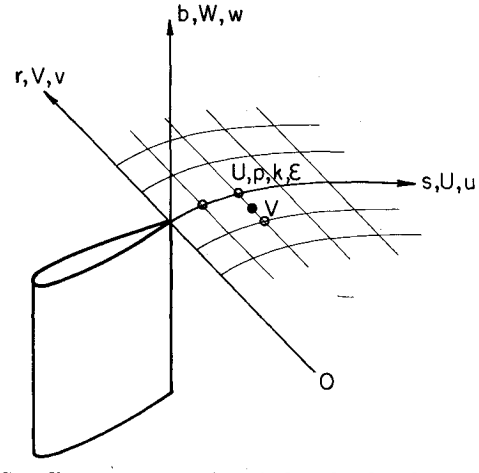

Fig. 1 Coordinate system and typical nodes for the wake of an airfoil.

and for the first model,

$$P=\nu_{\text{eff}}\left[2\left(\frac{\partial U}{\partial s}\right)^2+2\left(\frac{\partial V}{\partial r}\right)^2+\left(\frac{\partial U}{\partial r}\right)^2\right.$$
$$\left.+\left(\frac{\partial V}{\partial s}\right)^2+2\frac{\partial U}{\partial r}\frac{\partial V}{\partial s}-\frac{U}{r}\frac{\partial V}{\partial s}-\frac{U}{r}\frac{\partial U}{\partial r}\right]$$

The above expression can be further simplified for the thin shear layer with small pressure gradient in the normal direction,

$$P=\nu_{\text{eff}}\left[\left(\frac{\partial U}{\partial r}\right)^2-\frac{U}{r}\frac{\partial U}{\partial r}\right] \tag{10}$$

The second term of the above expression has the same form as the principal term of Eq. (8) and represents the curvature effect that was discussed qualitatively. As will be shown in the next section, the turbulence closure models with the conventional dissipation equation [with the source term, Eq. (5a)] does not predict curved turbulent wakes accurately even though the transport equations are in the curvilinear coordinate system. Referring to Eq. (3), it is clear that the turbulent kinetic energy increases with a decrease in angular momentum (rU). However, the dissipation rate also increases when the production of kinetic energy is used as the source term in the transport equation of the energy dissipation rate and the overall effect of curvature is not included adequately in the turbulence modeling.

Chambers and Wilcox[20] proposed modification of the first model for the curvature effect. They suggested modification to the turbulent kinetic energy equation by adding extra singular terms for the effects of streamline curvature. However, these modifications do not change the rate of energy dissipation adequately, and do not fully account for the curvature effect for the present set of data.

Two different dissipation equations were tried for better prediction of curved turbulent wakes. As Lumley and Khajeh-Nouri[21] argued, the production term can be used as source term in the dissipation equation with the assumption that

$$(\overline{u^iu^j}-\tfrac{2}{3}k\delta_{ij})\propto(U^i{}_{,j}+U^j{}_{,i})$$

This assumption is not valid when the flowfield is affected by streamline curvature and rotation; therefore, the exact source term

$$(\overline{u^iu^j}-\tfrac{2}{3}k\delta_{ij})\,(\overline{u^ju^i}-\tfrac{2}{3}k\delta_{ji})$$

by Lumley and Khajeh-Nouri[21] was utilized. To make the dimensions correct, the following source term was used for the present calculation:

$$S_2=C_\ell\frac{\epsilon^2}{k^3}(\overline{u^iu^j}-\tfrac{2}{3}k\delta_{ij})\,(\overline{u^ju^i}-\tfrac{2}{3}k\delta_{ji}) \tag{11}$$

which is given as the second form of the source term in Eq. (4).

Also, a modification of the conventional dissipation equation was tried to represent the curvature effect more accurately. The coefficient of the source terms which includes production of energy was modified as follows,

$$S_3=C_{\epsilon 1}(1+C_cR_i)(\epsilon/k)P \tag{12}$$

where

$$R_i=\frac{k}{\epsilon}\frac{1}{r}\frac{\partial(rU)}{\partial r}$$

and can be interpreted as the Richardson number in curved turbulent flow. The constant C_c relates the streamline curvature to the local dissipation rate, and the optimized value with the available data was 0.03.

Qualitative analysis of the effect of rotation on wake development was given by Lakshminarayana and Reynolds.[22] The total turbulent kinetic energy is not changed by rotation, but the kinetic energy is redistributed by the rotation when the turbulence is not isotropic. Hah and Lakshminarayana[19] included the effects of rotation on the turbulence structure in their calculation of turbulent wakes of rotor blades. The effect of rotation depends on the local structure of turbulence, and it is not sufficient to adopt a simple parameter (like the Rossby number) to represent this effect on the turbulence closure scheme. Therefore, no attempt was made to modify the first turbulence closure model for the effects of rotation.

The second and third closure models include the effect of rotation through the rotation-originated redistribution term in the transport equations of Reynolds stresses. Various turbulence closure models used for the present investigation are shown in Table 1.

Solution Algorithm

The continuity and mean momentum equations [Eqs. (1) and (2)] along with turbulence closure equations [Eqs. (3), (4), (6), or (7)] were solved in elliptic form. At the near weak region, the streamwise velocity gradient ($\partial U/\partial s$) is of the same order of magnitude as the normal velocity gradient ($\partial U/\partial r$) and none of the shear stress components are negligible. Therefore, the conventional boundary-layer assumption can not be invoked in this region. The parabolic marching technique does not produce accurate predictions. The initial values of unknowns were obtained by parabolic marching technique, then the values were corrected iteratively. A total of 120 nodal points were used in the normal direction for the wake of a single airfoil and cascade. Up to 216 nodal points were used in the normal direction for the three-dimensional wake of a rotor blade, and no wall function was utilized in the wake center region. The turbulence kinetic energy and the rate of energy dissipation were handled as diffusion terms in the first and second models. In the second model, the Reynolds stress components were first computed using Eq. (6) and the values of U^i, k, ϵ at the previous iteration. The governing equations were solved with these Reynolds stress components. Typical positions of grid nodes are shown in Fig. 1. In the third model, the shear stress nodes were located between the adjacent nodes in the normal direction to provide stability in calculation. About 20 iterations gave converged values for all closure models. Figure 2 shows calculated values at different iterations for the wake of a single airfoil with the second turbulence closure model.

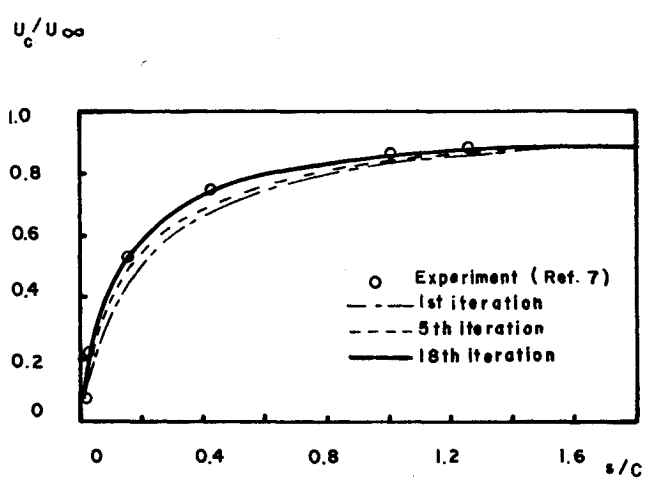

Fig. 2 Wake decay predictions at various iterations.

About 20 s were necessary for each iteration with the first model on IBM 370/3066 at The Pennsylvania State University. The second and third models require about 20 and 50% more computing time, respectively.

Predictions for the Wake of a Single Airfoil and Cascade

For the calculation of curved turbulent wakes of a single airfoil and cascade, the curvilinear coordinate system shown in Fig. 1 was used. r is the distance from the origin of curvature, s is the streamwise distance on the specified path, and n is normal to s and r. With this coordinate system, the actual streamline of wake can be closely represented. This coordinate system forms part of the coordinate system for the calculation of the wakes of the single airfoil and the cascade blade. The fundamental metric tensor for this coordinate system is

$$g_{ij}=\begin{bmatrix} 1 & -\frac{s}{r} & 0 \\ -\frac{s}{r} & 1+\frac{s^2}{r^2} & 0 \\ 0 & 0 & 1 \end{bmatrix} \qquad g^{ij}=\begin{bmatrix} 1+\frac{s^2}{r^2} & \frac{s}{r} & 0 \\ \frac{s}{r} & 1 & 0 \\ 0 & 0 & 1 \end{bmatrix} \tag{13}$$

Christoffel symbols of the second kind are as follows,

$$\Gamma^1_{11}=-\frac{s}{r^2},\quad \Gamma^2_{11}=-\frac{1}{r},\quad \Gamma^1_{12}=-\Gamma^2_{22}=\frac{s^2}{r^3}$$

$$\Gamma^2_{21}=\frac{s}{r^2},\quad \Gamma^1_{22}=-\frac{s^3}{r^4} \tag{14}$$

All other Christoffel symbols of the second kind are zero.

The comparison between measured and predicted characteristics of a wake was made using the data of Hah and Lakshminarayana.[7] The blade shape used in Ref. 7 was NACA 0012; the other parameters are: chord length of 0.2 m, Reynolds number of 3×10^5 based on chord length, 0.4% of freestream turbulence intensity. The measurement included mean values of streamwise and normal velocities and the Reynolds stress across the wake at various streamwise locations for several incidence angles. The inlet value of each dependent variable (except dissipation) was obtained from the experimental data. The dissipation was assumed to be equal to the production of turbulent kinetic energy at that location. The calculated profiles of velocity without curvature modification are given in Fig. 3a. The experimental data are given for comparison. The results with curvature modifications are also given in Figs. 3b and 3c. Comparison of shear stress is given in Fig. 4. The figures show that the three turbulence models do not predict the mean velocity and shear stress profiles accurately when the conventional dissipation equation with source term [Eq. (5a)] is used. All three models predict higher shear stress at pressure side and lower shear stress at suction side than experimental data. But this discrepancy between theory and experiment disappeared by modifying the coefficient of the conventional source term, Eq. (12), or by adopting the exact source term, Eq. (11). All three models predicted almost identical results for mean velocity and shear stress when the modified dissipation equation was used. The calculated values of turbulence intensities with three models are shown in Fig. 5. For the wake with streamline curvature, the first model predicted almost identical values for the three intensity components, and the profile was corrected when the modified or exact source term was used in the dissipation equation.

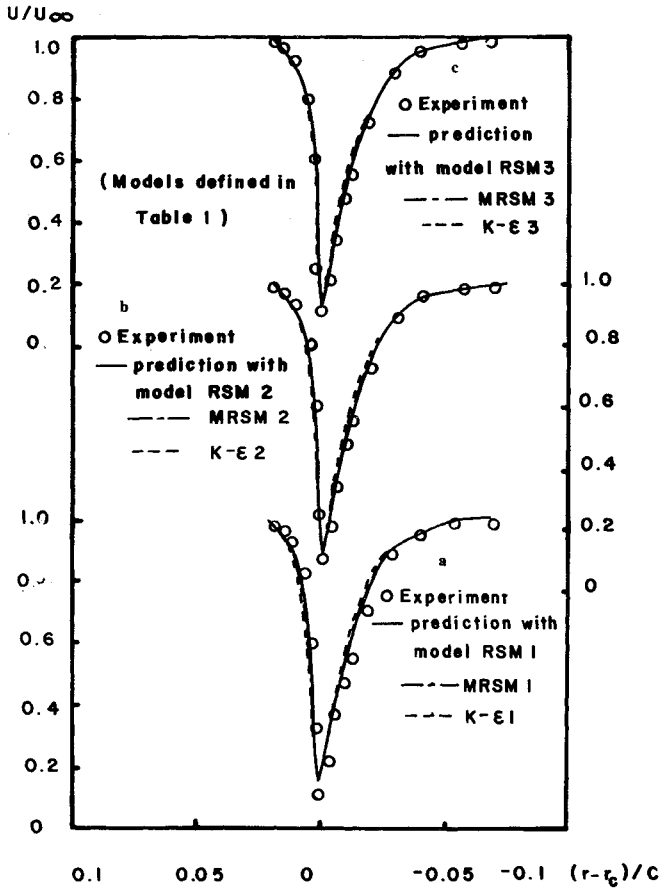

Fig. 3 Streamwise velocity profile for an isolated airfoil wake at $s/C=0.03$. Experimental data from Ref. 7. Refer to Table 1 for details of various turbulence models used.

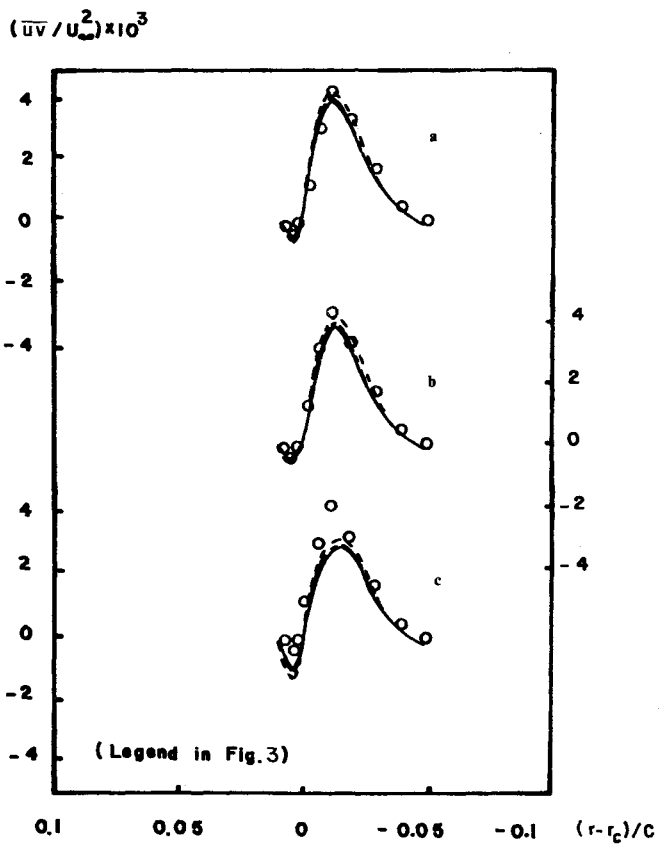

Fig. 4 Shear stress profile for an isolated airfoil wake at $s/C=0.03$. Experimental data from Ref. 7.

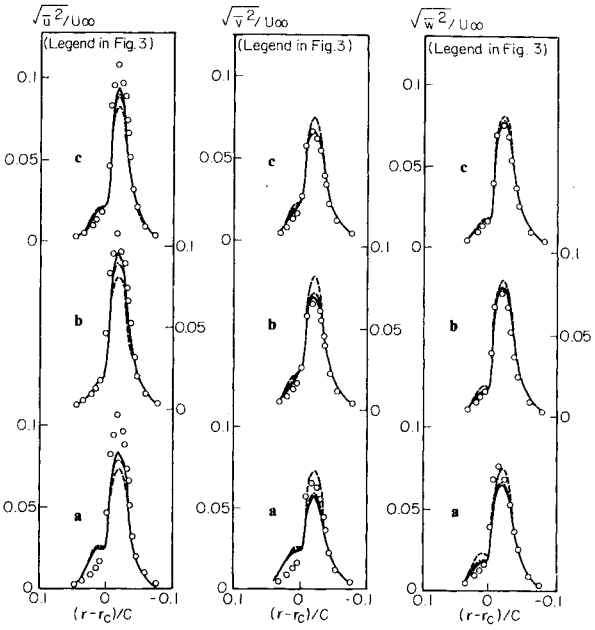

Fig. 5 Relative turbulence intensity profiles for an isolated airfoil wake at $s/C=0.03$. Experimental data from Ref. 7.

The second and third turbulence closure models with conventional dissipation equation [with source term of Eq. (5a)] predict a higher intensity level in the pressure side and a lower intensity level in the suction side than do the experimental data. However, the discrepancy between prediction and experiment was considerably decreased by modifying the coefficient of the conventional source term or by adopting the exact source term. As discussed previously, the production of turbulent kinetic energy cannot be used as a source term in the dissipation equation, especially for the turbulent flow with streamline curvature.

The wakes of a cascade measured by Raj and Lakshminarayana[23] were calculated for further comparison. The blade profiles were similar to the NASA-65 ($8A_2I_{8b}$) 10 blade section, and other important parameters are; solidity $C/S=1.505$, inlet angle $\beta_1=45$ deg, incidence $i=6$ deg, and Reynolds number based on chord $=3\times10^5$. The upstream velocity and freestream intensity were 24 ms^{-1} and 0.16%. Because the experimental data did not provide spanwise intensity, the energy distribution at inlet boundary was guessed with available single airfoil wake data. Also, the rate of turbulent kinetic energy dissipation was assumed to be equal to the production of energy. Because of the characteristics of the flow around a cascade, the periodic boundary condition was applied between corresponding points in normal directions; the flowfield and coordinate system are shown in Fig. 6. Figures 7a-c show predicted mean velocity distribution with three turbulence models. The comparison of shear stress is given in Fig. 8. The modified turbulence closure models show substantial improvement in prediction compared to original closure models, and all three of the models predict almost identical results if they are properly modified. The predicted intensity distributions are shown in Fig. 9. The first model predicted only isotropic intensity values, although the trend was improved by modifying the conventional source term for curvature or adopting the exact source term in the dissipation equation. The second and third models provided better predictions for individual components, and improvements were observed when the dissipation equation was modified. The discrepancy between theory and experiment in the distribution of streamwise intensity near the center of the wake is not explained at this stage. It may be due to scattering in measurements or to improper turbulence modeling. The trajectory of wake centerline is shown compared with

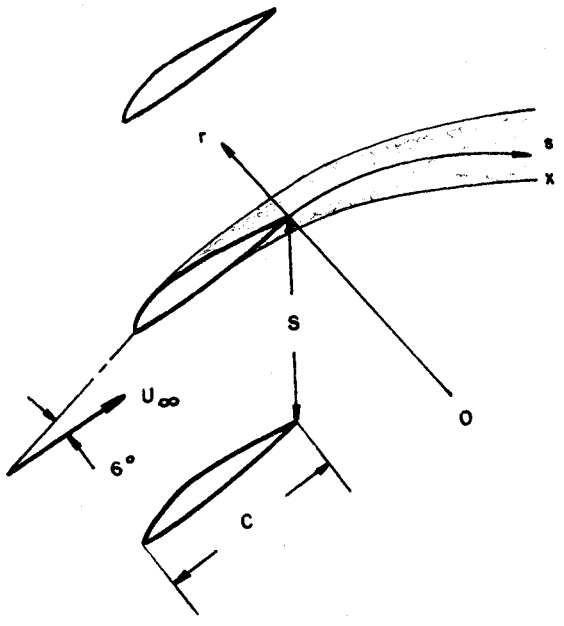

Fig. 6 Coordinate system for the wake of a cascade.

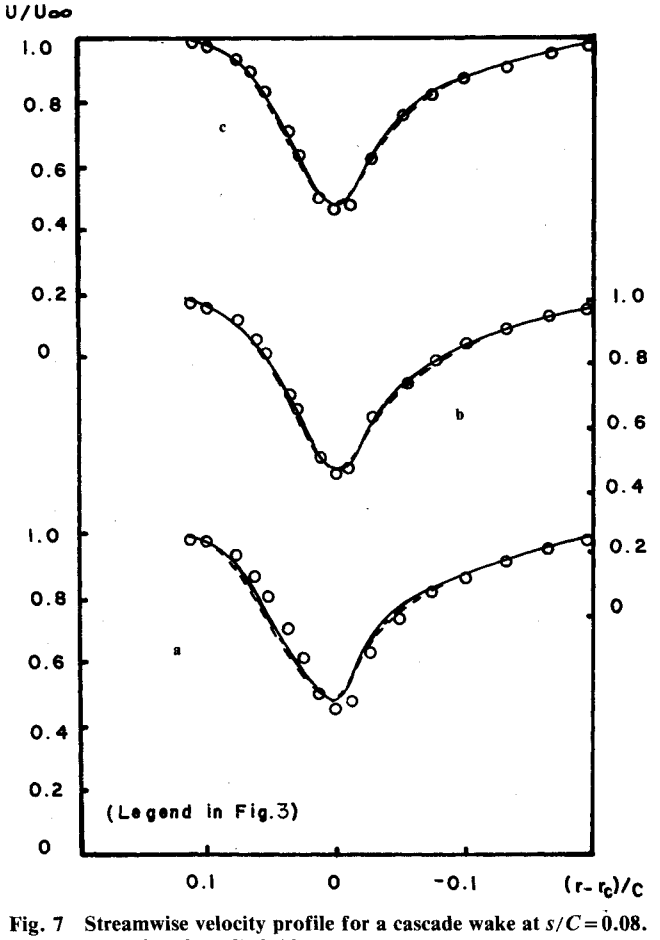

Fig. 7 Streamwise velocity profile for a cascade wake at $s/C=0.08$. Experimental data from Ref. 23.

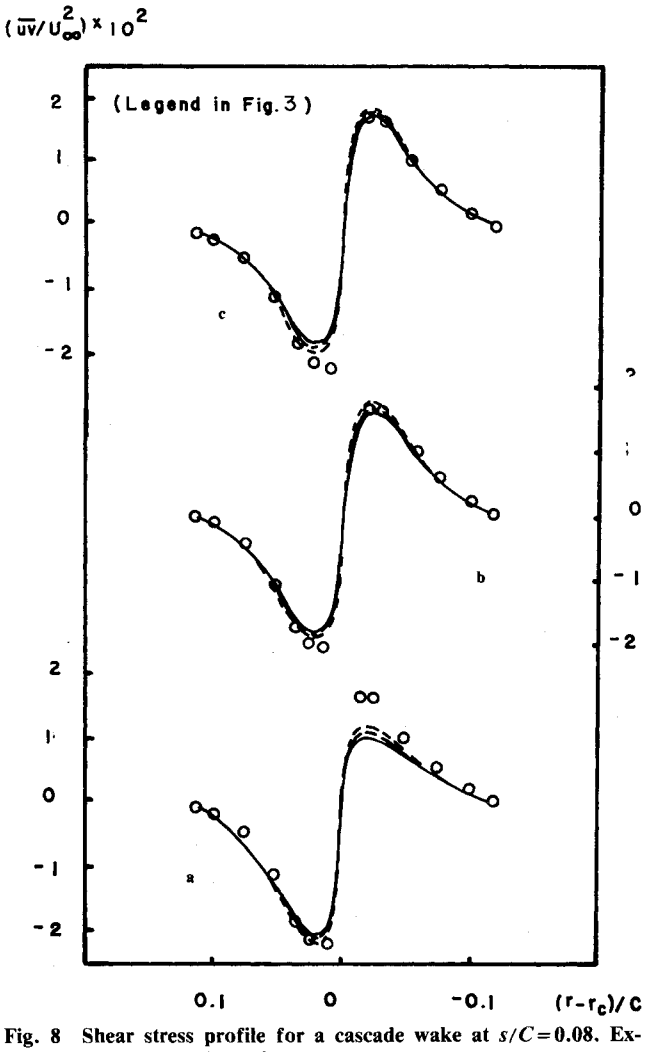

Fig. 8 Shear stress profile for a cascade wake at $s/C=0.08$. Experimental data from Ref. 23.

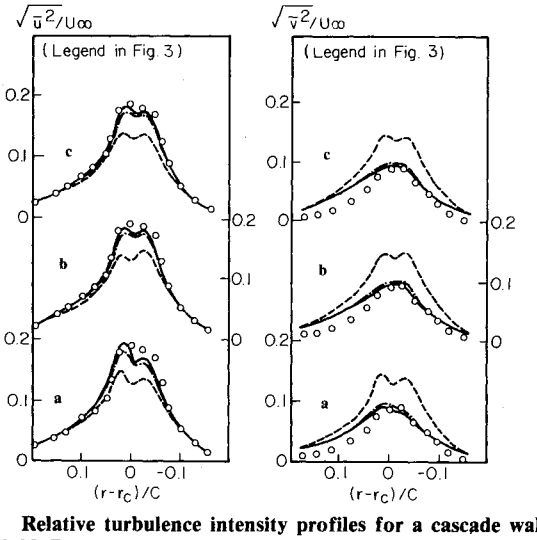

Fig. 9 Relative turbulence intensity profiles for a cascade wake at $s/C=0.08$. Experimental data from Ref. 23.

predicted values in Fig. 10. Even though the curvature seems moderate, its effect on turbulence structure as well as mean velocity is appreciable.

Prediction for the Wake of Rotor Blades

To compare the performances of turbulence closure models for the combined effects of streamline curvature and rotation, the three-dimensional wakes of rotor blades were computed. The flowfield and coordinate system are given in Fig. 11. The radial velocity component is generated by centrifugal and Coriolis forces in the boundary layer. The detailed derivation of governing equations in this coordinate system and numerical calculations with conventional dissipation equation are given by Hah and Lakshminarayana.[19] For general three-

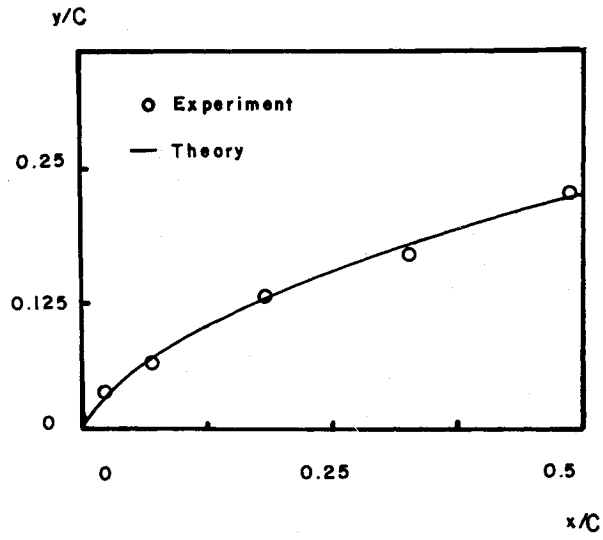

Fig. 10 Locus of wake center (minimum velocity) for a cascade. Experimental data from Ref. 23.

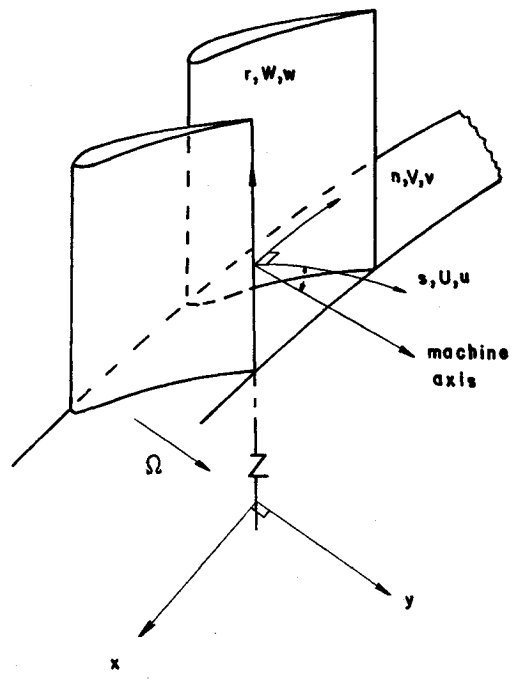

Fig. 11 Coordinate system for the calculation of turbomachinery rotor wake.

dimensional flow, nine components of curvature exist. For flows with multiple components of curvature, the correction method with simple parameter, Eq. (12) cannot be used. Three major components of curvature are considered for the present flow, because the flow develops approximately on the helical path on the cylinder as shown in Fig. 11. One is due to machine radius, and this component dominates when the boundary-layer thickness on the blade is large compared to the machine radius. The second is the curvature of the streamline on the cylindrical surface, and this component was mainly considered in the calculation of the wake of a single airfoil and cascade. The third component of curvature is due to the radial variation of angle β of Fig. 11. For practical shape of compressors, this component cannot be neglected. The predictions with the conventional dissipation equation [with the source term, Eq. (5a)] and the prediction with exact source term in the dissipation equation (11) are compared for the combined effects of the streamline curvature and rotation. Because of the limitations of computer storage, the third turbulence closure model was not tried for the prediction of this flow and the comparison was made with only the first and second models.

The experimental data by Ravindranath and Lakshminarayana[15] were used for comparison. The experiment was done in a single-stage compressor with moderately loaded blades. Some relevant data on the compressor and the operating conditions are; hub/tip ratio = 0.5, rpm = 1066, number of blades = 21, incidence at midradius = 7 deg, stagger angle at midradius = 50 deg, ratio of blade chord to spacing at midradius = 0.6. Ten radial stations were used to calculate the flowfield and the periodic boundary condition was applied. The measured values were used as the boundary condition of elliptic calculation. About 20 iterations gave reasonable convergency and the computing time was up to 30 min. Figures 12 and 13 show the calculated profile of mean velocity. These results indicate that both the streamline curvature and rotation affect the development of the wake. The first model, which does not include the rotation effect in modeling, does not predict accurate values even if the cur-

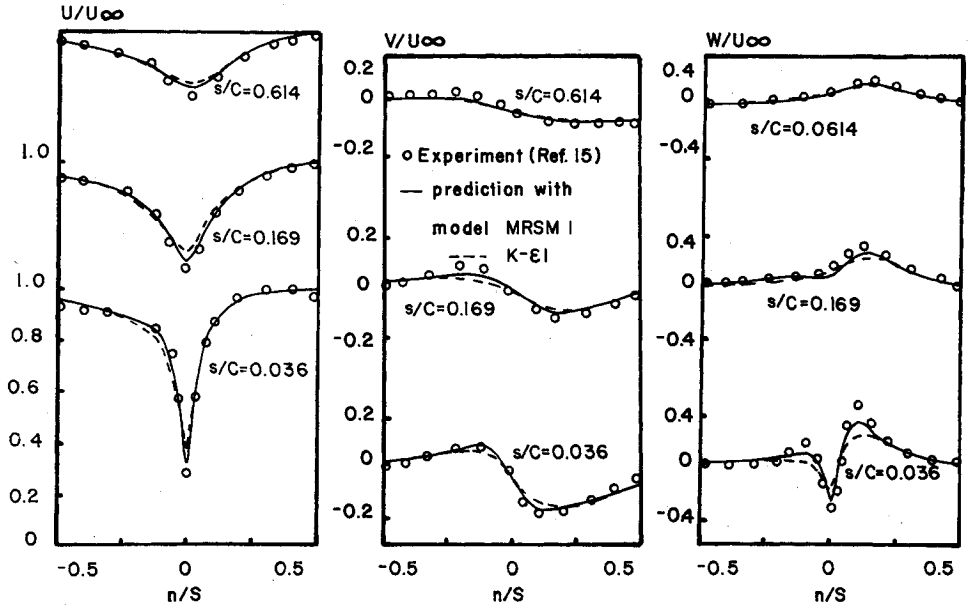

Fig. 12 Profiles of mean velocity components for a rotor blade wake at $r/r_t = 0.8$. Experimental data from Ref. 15.

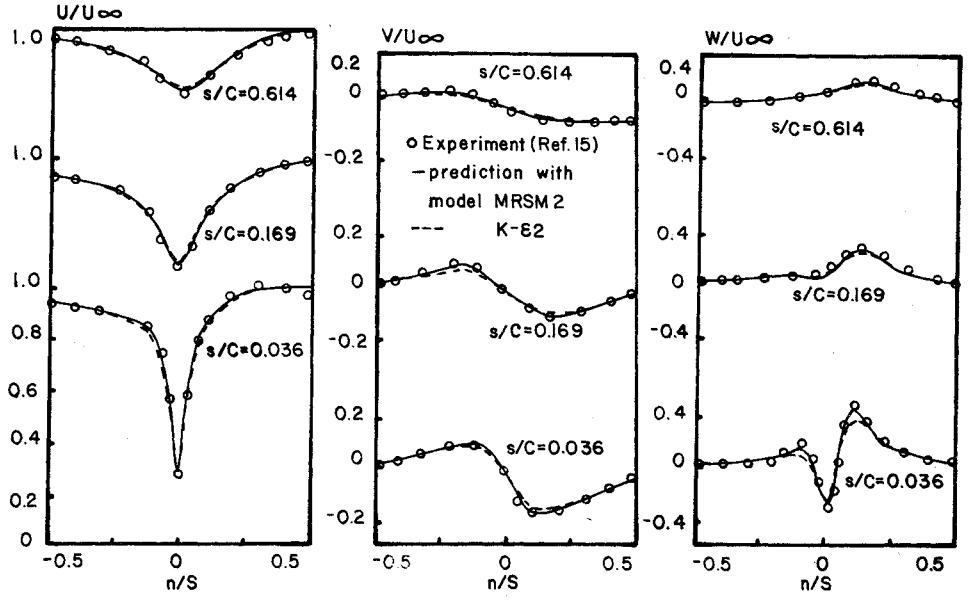

Fig. 13 Profiles of mean velocity components for a rotor blade wake at $r/r_t = 0.8$. Experimental data from Ref. 15.

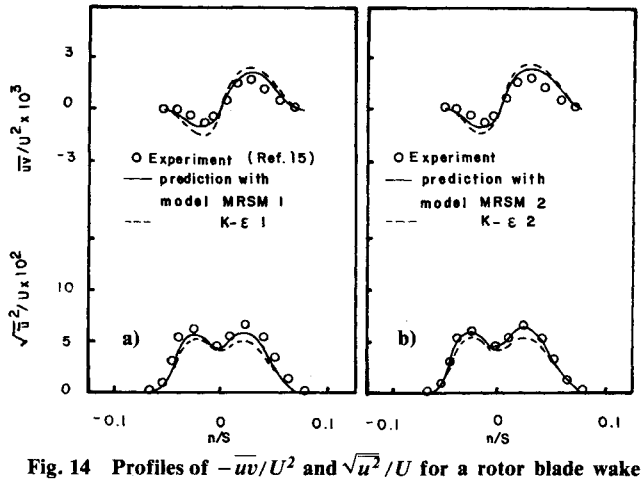

Fig. 14 Profiles of $-\overline{uv}/U^2$ and $\sqrt{\overline{u^2}}/U$ for a rotor blade wake at $r/r_t = 0.8$. Experimental data from Ref. 15.

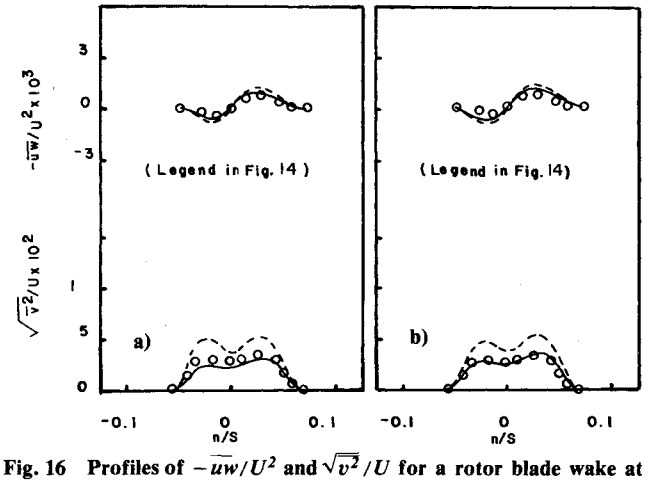

Fig. 16 Profiles of $-\overline{uw}/U^2$ and $\sqrt{\overline{v^2}}/U$ for a rotor blade wake at $r/r_t = 0.8$. Experimental data from Ref. 15.

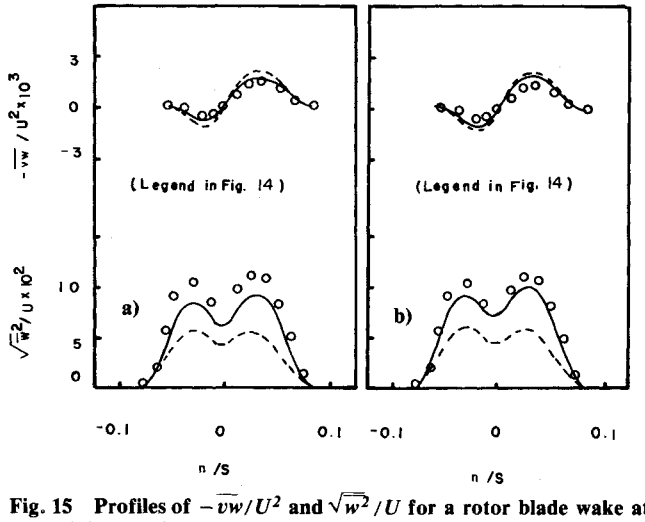

Fig. 15 Profiles of $-\overline{vw}/U^2$ and $\sqrt{\overline{w^2}}/U$ for a rotor blade wake at $r/r_t = 0.8$. Experimental data from Ref. 15.

vature effect is included. Figures 14-16 show the calculated distributions of Reynolds stress. Here again, the first model does not predict individual intensity components. The second turbulence closure model predicted quite accurate values of all Reynolds stress components.

Concluding Remarks

Two- and three-dimensional asymmetrical turbulent wakes were calculated numerically with three different turbulence closure models. The transport equation for the rate of turbulent kinetic energy dissipation was modified to represent the effect of streamline curvature. The exact form of the source term in the dissipation equation was used in place of the conventional production term for curved flow. Also, the coefficient of the conventional source term was modified to represent the curvature effect. The effect of rotation was included in the calculation through the rotation-originated redistribution term in the transport equation of Reynolds stress. The first model was not modified for the effect of rotation. The calculated results show that the curvature effect can be properly included by all three models and the mean velocity and shear stress can be predicted accurately with these models. For the flow which develops under the effect of rotation, the second and third models predicted better results as compared to the first model.

Acknowledgments

This work was supported by the National Aeronautics and Space Administration through Grant NSG 3012, with M. F. Heidmann as the Technical Monitor.

References

[1]Launder, B. E., Reece, G. J., and Rodi, W., "Progress in the Development of a Reynolds-Stress Turbulence Closure," *Journal of Fluid Mechanics*, Vol. 68, April 1975, pp. 537-566.

[2]Pope, S. B. and Whitelaw, J. H., "The Calculation of Near-Wake Flows," *Journal of Fluid Mechanics*, Vol. 73, Jan. 1976, pp. 9-32.

[3]Prandtl, L., "Einfluss stabilisierender Kräfte auf die Turbulenz," Souderdruck aus Vostrage aus dem Gebiete der Aerodynamik und Verwandter Gebiete, Aachen, 1929 (Translation NACA TM-625).

[4]Patel, V. C., "The Effects of Curvature on the Turbulent Boundary Layer," Aeronautic Research Council, R&M No. 3599, Aug. 1969.

[5]So, R.M.C. and Mellor, B. L., "An Experimental Investigation of Turbulent Boundary Layers Along Curved Surfaces," NASA Contractor Rept. 1940, 1972.

[6]Castro, I. P. and Bradshaw, P., "The Turbulence Structure of a Highly Curved Mixing Layer," *Journal of Fluid Mechanics*, Vol. 73, Feb. 1976, pp. 265-304.

[7]Hah, C. and Lakshminarayana, B., "Experimental and Numerical Study of Asymmetrical Wakes of a Single Airfoil," in preparation.

[8]Bradshaw, P., "Effects of Streamline Curvature on Turbulent Flow," AGARDograph No. 169, 1973.

[9]So, R.M.S., "A Turbulent Velocity Scale for Curved Shear Flows," *Journal of Fluid Mechanics*, Vol. 70, Jan. 1975, pp. 37-58.

[10]Bradshaw, P., "The Analogy Between Streamline Curvature and Buoyancy in Turbulent Shear Flow," *Journal of Fluid Mechanics*, Vol. 36, June 1969, pp. 177-191.

[11]Launder, B. E., Pridden, C. H. and Sharma, B. I., "The Calculation of Turbulent Boundary Layers on Spinning and Curved Surfaces," *Transactions of ASME, Journal of Fluid Engineering*, Vol. 99, March 1977, pp. 231-239.

[12]Johnston, J. P., "The Effects of Rotation on Boundary Layers in Turbomachine Rotors," NASA SP-304, edited by B. Lakshminarayana et al., 1974.

[13]Raj, R. and Lakshminarayana, B., "Three-Dimensional Characteristics of Turbulent Wakes Behind Rotors of Axial-Flow Turbomachinery," *Transactions of ASME, Journal of Engineering for Power*, Vol. 98, April 1976, pp. 218-228.

[14]Reynolds, B., Lakshminarayana, B., and Ravindranath, A., "Characteristics of the Near-Wake of a Compressor or Fan Rotor Blade," *AIAA Journal*, Vol. 17, Sept. 1979, pp. 959-967.

[15]Ravindranath, A. and Lakshminarayana, B., "Mean Velocity and Decay Characteristics of the Wake of a Compressor Blade with Moderate Loading," submitted for publication in the *Journal of Engineering for Power*, Vol. 102, No. 3, July 1980, pp. 535-548.

[16]Majumdar, A K., Pratrap, V. S., and Spalding, D. B., "Numerical Computation of Flows in Rotating Ducts," *Transactions of ASME, Journal of Fluid Engineering*, Vol. 99, March 1977, pp. 148-153.

[17]Rotta, J. C., "Statische thorie nichthomogener turbulenz," *Journal of Physics*, Vol. 129, 1976, p. 547.

[18]Naot, D., Shavit, A., and Wolfshtein, M., "Interactions between Components of the Turbulent Velocity Correlation Tensor," *Israel Journal of Technique*, Vol. 8, 1970, p. 259.

[19]Hah, C. and Lakshminarayana, B., "Numerical Analysis of Turbulent Wakes of Axial Flow Turbomachinery Rotor Blades," *Proceedings, Symposium on Turbulent Boundary Layers*, edited by H. E. Weber, American Society of Mechanical Engineers, 1979.

[20]Chambers, T. L. and Wilcox, D. C., "Critical Examination of Two-Equation Turbulence Closure Models for Boundary Layers," *AIAA Journal*, Vol. 15, June 1977, pp.

[21]Lumley, J. L. and Khajeh-Nouri, B., "Computational Modeling of Turbulent Transport," *Advances in Geophysics*, Vol. A18, 1974, pp. 169-192.

[22]Lakshminarayana, B. and Reynolds, B., "Turbulence Characteristics in the Near Wake of a Compressor Rotor Blade," AIAA Paper 79-0280, 1979.

[23]Raj, R. and Lakshminarayana, B., "Characteristics of the Wake Behind a Cascade of Airfoils," *Journal of Fluid Mechanics*, Vol. 61, Dec. 1973, pp. 707-730.

From the AIAA Progress in Astronautics and Aeronautics Series . . .

INJECTION AND MIXING IN TURBULENT FLOW—v. 68

By Joseph A. Schetz, Virginia Polytechnic Institute and State University

Turbulent flows involving injection and mixing occur in many engineering situations and in a variety of natural phenomena. Liquid or gaseous fuel injection in jet and rocket engines is of concern to the aerospace engineer; the mechanical engineer must estimate the mixing zone produced by the injection of condenser cooling water into a waterway; the chemical engineer is interested in process mixers and reactors; the civil engineer is involved with the dispersion of pollutants in the atmosphere; and oceanographers and meteorologists are concerned with mixing of fluid masses on a large scale. These are but a few examples of specific physical cases that are encompassed within the scope of this book. The volume is organized to provide a detailed coverage of both the available experimental data and the theoretical prediction methods in current use. The case of a single jet in a coaxial stream is used as a baseline case, and the effects of axial pressure gradient, self-propulsion, swirl, two-phase mixtures, three-dimensional geometry, transverse injection, buoyancy forces, and viscous-inviscid interaction are discussed as variations on the baseline case.

200 pp., 6×9, illus., $17.00 Mem., $27.00 List

TO ORDER WRITE: Publications Dept., AIAA, 1290 Avenue of the Americas, New York, N. Y. 10019